Journal of Materials Chemistry B

Accepted Manuscript

ROYAL SOCIETY OF CHEMISTRY

www.rsc.org/materialsB

Journal of Materials Chemistry B RSCPublishing

PAPER

Oligonucleotides as 'bio-solvent' for *in situ* extraction and functionalisation of carbon nanoparticles

Cite this: DOI: 10.1039/x0xx00000x

Yu-Cheng Chen, Cheng-Che Wen, Ian Liau, You-Zung Hsieh and Hsin-Yun Hsu*

Received 00th January 2014,
Accepted 00th January 2014

DOI: 10.1039/x0xx00000x

www.rsc.org/

A simple yet novel one-pot approach is developed to prepare carbon nanoparticles with diameters of ~2 nm and modified by oligonucleotides. We use single-stranded deoxyribonucleic acid (ssDNA), which serves as a unique 'bio-solvent' for carbon nanoparticle (CNP) preparation and as a target molecule for functionalisation. Proposed interactions relevant to the stabilisation of the final oligonucleotide–CNP complex include π–π stacking and π–HN bonding with sp^2 carbon atoms on the CNP surface. Furthermore, oligonucleotide-enriched CNPs can be readily extracted within seconds from a crude mixture of single-walled carbon nanotubes (SWCNTs) without any need for post-synthesis chemical modification. The established CNPs are biocompatible, possess intrinsic fluorescence, and do not result in the undesirable photobleaching effect, rendering them potential candidates for *in vivo* biological applications.

Introduction

The diverse family of nanocarbons, which includes nanometer-sized amorphous carbon, fullerenes, diamondoids, and tubes, has been applied extensively to the development of drug-delivery systems, bioimaging probes, and sensors. Single-walled carbon nanotubes (SWCNTs) with average diameters of 0.7–1.1 nm,[1] fabricated by high-pressure decomposition of carbon monoxide (also called the HiPco process), allow visible-light excitation and the detection of fluorescence at near-infrared (NIR) wavelengths in the range of 900–1400 nm.[2,3] This optical property allows SWCNTs to be characterised effortlessly and applied as detection probes in laboratories with common spectrophotometric instruments.[4–6] On the other hand, quantum-sized (1–10 nm) carbon nanoparticles (CNPs), fabricated by various methods, possess inherent fluorescence and thus appear to be a promising alternative material in various bio-applications.[7–12] They are also environmentally benign with negligible toxicity and are considerably cost-effective compared to semiconductor quantum dots (QDs). A well-known example is the nanocrystalline diamond (ND), which exhibits excellent mechanical and optical properties and is therefore suitable for a diverse range of imaging modalities *in vitro* and *in vivo*.

In order to fully exploit these versatile materials, several challenging requirements must be met, however, including attaining precise control of the particle size, shape, dispersity, and surface chemistry during nanocarbon synthesis. The processes used to fabricate SWCNTs and CNPs offer both advantages and disadvantages. Although the HiPco process SWCNTs generates more defects in the grown SWCNTs than other methods, which may facilitate subsequent surface modification,[13–15] the aggregation of isolated nanotubes and acidification during synthesis reduce the photoluminescence (PL) intensity dramatically.[16] The production of ND often involves a detonation method, while amorphous CNPs can be prepared using a variety of techniques including laser ablation of graphite,[17] electro-oxidation of graphite,[18] treatment of carbon precursors with HNO_3,[19] and hydrothermal decomposition of organic compounds.[20] A well-known example is presented in the work of Liu *et al.*,[7] who treated the carbon precursor with HNO_3, followed by 12h of refluxing, centrifugation, neutralisation, and dialysis to purify the end products. Xu and co-workers[8] employed electrophoresis to separately enrich carbon nanotubes of different lengths and fluorescent nanoparticles. Several research groups[2,21,22] have also taken advantage of the π–π interaction between oligonucleotides and carbon-based materials to immobilise diverse DNA sequences for the synthesis of novel nanoconjugates. However, all reported strategies were complex and involved multiple surface-modification steps; most of the modifications often required specific ligand functionalisation, which entailed various rounds of physical and chemical processing.

To address these challenges, we focused our efforts on exploiting the strong π–π stacking interactions displayed between sp^2 carbon atoms on the surfaces of carbon nanomaterials[23] and biopolymer nucleobases. The present study reports our findings in the development of a novel approach comprising oligonucleotide-facilitated extraction of fluorescent CNPs from synthesised SWCNTs. Using chemical vapour deposition (CVD), the initial SWCNTs were prepared with diameters $\lesssim$2 nm. Our study indicates that the extraction efficiency of CNPs largely depends on the nucleobase composition. Furthermore, the presence of π–HN interactions can act as an additional force in stabilising the final oligonucleotide–CNP complex. To the best of our knowledge, this is the first time the interaction of nucleobases with such small CNPs has been studied. We demonstrated that oligonucleotides may serve as a 'bio-solvent' for isolation and as ligands for functionalisation of CNPs, making them a highly efficient, eco-friendly, and biocompatible fluorescence probe. While there are no prior reports of direct application of biomolecules to isolate and functionalise fluorescent CNPs from acid-treated-SWCNT precursors, we succeeded in showing that oligonucleotide-modified CNPs can be readily enriched and purified in a single step, eliminating the

complex synthesis processes that have been previously reported. In addition, the photostable fluorescence of these CNPs should make them suitable for new applications in biological systems.

Experimental

Characterisation of CNPs

In a typical procedure to prepare the CNPs, 20 mg of SWCNTs (Centron Biochemistry Technology Co., Taiwan) were mixed by sonication into a 20 mL solution of H_2SO_4 and HNO_3 (3:1, v/v) for 8h. After centrifugation (5,000 × g (rcf) for 10 min), the supernatant was discarded, and the precipitate was re-suspended, washed with double-distilled water (ddH_2O) to reach an approximately physiological pH of 7.0, and subsequently freeze-dried. Finally, CNPs were extracted and collected by the addition of $d(AT)_{15}$ oligonucleotide in various concentrations (incubated for 1 min prior to separation): 0.1, 1, 10, and 100 μM. To examine the extraction efficiency of various nucleobases, single-stranded deoxyribonucleic acid (ssDNA) consisting of the sequence $d(A)_{12}$, $d(T)_{12}$, $d(C)_{12}$, or $d(G)_{12}$ was prepared to a final concentration of 100 μM, allowing for the purification of carbon nanoparticles. Analysis by transmission electron microscopy (TEM) and X-ray photoelectron spectroscopy (XPS) were performed by pipetting 2 μL of the CNP solution onto a glass slide and drying the slide at room temperature. The specimens were analysed and mapped using a high-resolution transmission electron microscope (HRTEM; JEOL, JEM-2100, Japan), and the size of nanoparticles was manually analysed from the TEM image using the open-source processing software Image J. XPS was performed using Microlab 350 (VG Scientific, UK).

All Raman spectra were obtained using a customised in-house system. A HeNe laser (632.8 nm, JDS Uniphase, USA) was employed as the excitation source, and the power was set to 1.59 mW. The laser was coupled with an inverted optical microscope (IX71, Olympus, Japan) and focused onto the sample with an objective numerical aperture of 1.4 (UPLSAPO 100X, Olympus, Japan). The resulting signal was processed using a spectrograph (Spectra Pro-2300i, Princeton Instrument, USA) equipped with a grating consisting of 600 lines/mm and a cooled charge-coupled device (CCD; PIXIS 100, Princeton Instrument, USA). The samples (dispersed SWCNTs (1 mg) and extracted CNP solution (2 μL)) were placed in a glass-bottomed petri dish (MatTek, USA) to collect the spectral data. All processed spectra were subtracted from the baseline using polynomial fitting. Direct detection of CNP-emitted fluorescence was performed by excitation of the CNP solution under a blue-light (470 nm) illuminating box (ECX-F20, VilberLourmat, France). The detailed fluorescent spectra were then measured using a fluorescence spectrophotometer (F700, Hitachi, Japan). A full scan of excitation and emission at wavelengths in the range of 200–900 nm was obtained to construct the final 3D fluorescence spectra. The quantum yield of the CNPs was calculated according to the following equation:

$$\varphi = \varphi_R \frac{I}{I_R}\frac{OD_R}{OD}\frac{n^2}{n_R^2}$$

where φ is the quantum yield, I is the measured integrated emission intensity, OD is the optical density, and n is the refractive index. The subscript R represents the known fluorophore reference (*e.g.* quinine sulfate: $\varphi = 0.54$ in 0.1 M H_2SO_4).

For the thermal stability tests, the CNP solution extracted with the aid of oligonucleotide (100 μM) was heated and incubated in a water bath at 95 °C. The fluorescence intensity of CNPs was measured at 6-min intervals for 1 h. To test for any potential bleaching effect, the CNP solution was subjected to continuous fluorescent (18-W lamp, 380–760 nm) exposure for 2 weeks, and the resulting fluorescence intensity was measured using a fluorescence microplate reader (FLX 800, BioTek, USA).

In vitro cellular response of CNPs

Confocal laser-scanning microscopy (CLSM): Human colorectal carcinoma (HCT116) cells were prepared at a concentration of ~5 × 10^5 cells/mL in Dulbecco's modified Eagle medium (DMEM). Next, 300 μL of the cell suspension was incubated with 20 μL of the extracted CNPs solution for 2 h. After incubation, the HCT116 cells were rinsed twice with DMEM to remove any free CNPs and then refilled to refresh the final solution. The labelling cells were analysed for fluorescence using a confocal laser-scanning microscope (FV300, Olympus, Japan). For the 3-(4,5-dimethylthiazol-2-yl)-2,5 diphenyl tetrazolium bromide (MTT) assay, the HCT116 cells (concentration ≈ 10^4 cells/mL, 95 μL) were incubated with 5 μL of extracted CNPs solution under a stream of 5% CO_2 at 37 °C and monitored after 12, 24, and 36 h to evaluate their cytotoxicity. The collected cell suspensions were then reacted with 50 μL of an MTT solution (5 mg/mL) for 1 h, and the resulting absorbance was measured at 570 nm.

Results and Discussion

The workflow for the preparation of oligonucleotide-modified CNPs is summarised in Scheme 1. SWCNTs were treated with a solution of H_2SO_4 and HNO_3 (3:1, v/v))[24] under sonication for 8 h before the addition of an oligonucleotide solution [$d(AT)_{15}$] (this sequence was selected owing to its reported high affinity with SWCNTs[2]). Final extraction of fluorescent CNPs was accomplished by collecting the supernatant after 1 min of incubation. The supernatant displayed a colour change from transparent to beige, indicating that the CNPs were enriched and fabrication of the desired oligonucleotide-capped CNPs was successful. Fig. 1 shows representative images of the isolated CNPs obtained using HRTEM. The CNPs were approximately 2.1 ± 0.5 nm in size and amorphous in appearance, with no apparent crystalline features.

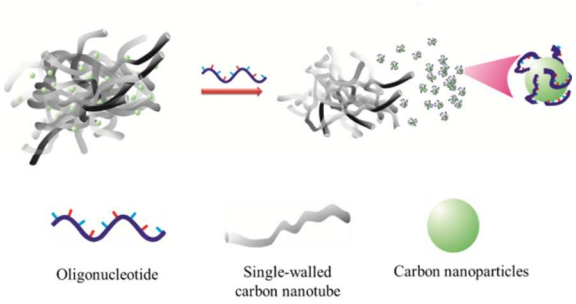

Scheme 1 Proposed scheme for oligonucleotide-facilitated *in situ* extraction and functionalisation of carbon nanoparticles.

Raman spectroscopy was employed to characterise the CNPs, and the results are shown in Fig. 2. The SWCNTs exhibited two characteristic bands, denoted as D and G within the Raman spectra.[8] The D band (near 1350 cm^{-1}) corresponds to the vibration of carbon atom bonds, which are expected to suspend in a disordered graphitic sp^2 network; the G band at 1593 cm^{-1} corresponds to the E_{2g} in-plane stretching vibration mode (C–C bonds of sp^3 hybridised C). The Raman spectra of functionalised CNPs appeared featureless, with almost indiscernible D and G bands, presumably owing to the intense background photoluminescence, which may have masked the D and G bands. More importantly, these results are consistent with those reported for other synthesised CNPs.[8]

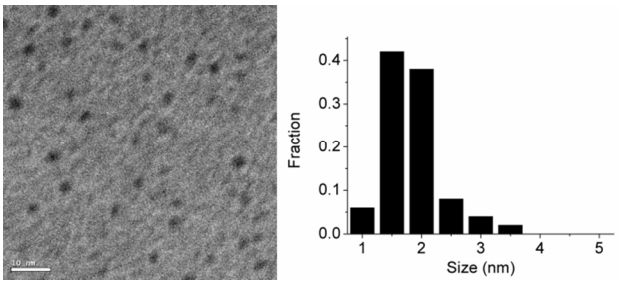

Fig. 1 HRTEM images of extracted CNPs. The size of a single CNP is approximately 2.1 ± 0.5 nm (manually analysed using Image J).

In order to confirm the presence of immobilised oligonucleotide-CNPs compared to native and unmodified forms, we synthesised a fluorescein FAM-labelled oligonucleotide (FAM-oligo), which comprised an identical sequence as the native oligo. Both the modified and native forms were tested for fluorescence. Because CNPs have been previously reported as a quencher of fluorescein,[25] we expected the immobilised FAM-oligo on CNPs to exhibit reduced fluorescence intensity. The corresponding fluorescence spectra of the free FAM-oligo probe and the CNPs modified by FAM-oligo (FAM-oligo-CNPs) are shown in Fig. 3.

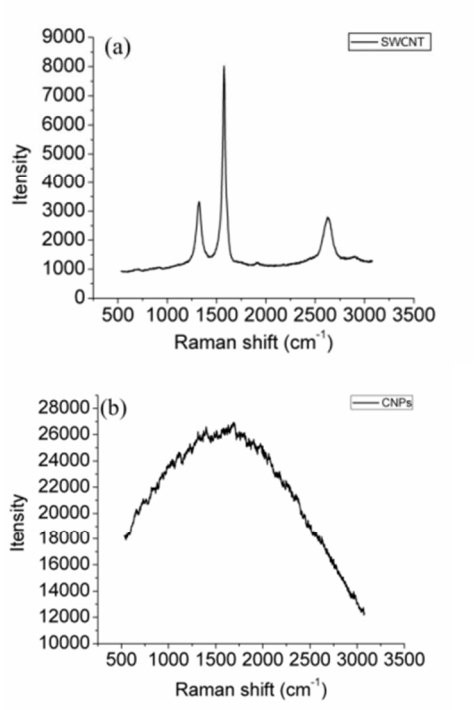

Fig. 2 Raman spectra of (a) SWCNTs and (b) functionalised fluorescent CNPs.

For the FAM-oligo sample, an intense emission band was observed at 520 nm (λ_{ex} = 495 nm). In contrast, for the FAM-oligo-CNPs, a similar emission peak was observed, but it had weaker intensity, presumably because of quenching of FAM resulting from electron transfer as FAM-oligo was absorbed onto the CNPs (Fig. 3a). Interestingly, an additional emission band at 446 nm (λ_{ex} = 350 nm) was detected for the FAM-oligo-CNP samples, which has been previously attributed to the intrinsic fluorescence exhibited by CNPs[25] and was absent in the FAM-oligo sample (Fig. 3b). Analysis using X-ray photoemission spectroscopy (XPS) (Fig. 4) further confirmed the chemical nature of the observed features of the CNPs. XPS data of the oligonucleotide-coated CNPs showed a spectral pattern analogous to previously reported oligonucleotide-modified SWCNTs.[26] To further investigate the photoluminescent properties of CNPs, a full scan of both the excitation and emission wavelength (from 200 to 900 nm) was performed to yield the 3D fluorescence spectra. As a result, we found that the maximal excitation wavelength of CNPs was located near 300 nm, and the corresponding maximal emission wavelength was ~450 nm (Fig. 5); a direct correlation was observed between the emission spectra and applied excitation wavelength. The quantum yield of the synthesised CNPs was determined to be 0.82%.

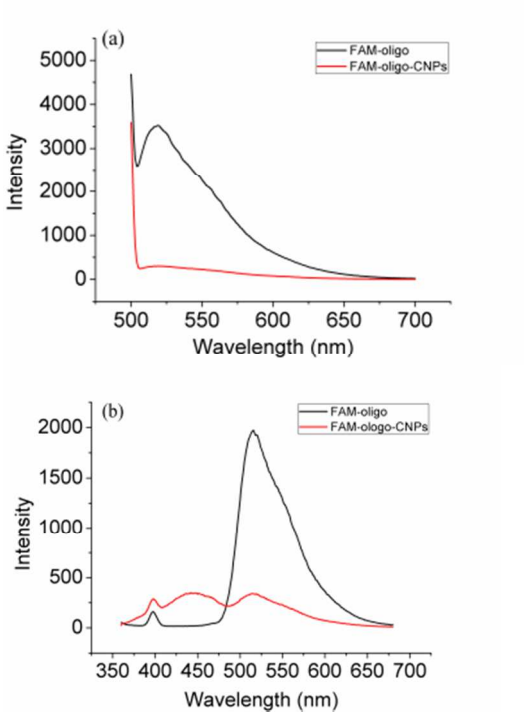

Fig. 3 Fluorescence spectra of FAM-labelled oligonucleotides (FAM-oligo) and CNPs modified with FAM-oligonucleotides (FAM-oligo-CNPs). (a) With excitation at 495 nm, an intense emission band near 520 nm was observed in the FAM-oligo sample; the FAM fluorescence was quenched in the sample of FAM-oligonucleotides-modified CNPs. (b) When the excitation wavelength was 350 nm, the FAM-oligo-CNPs showed an additional emission band at 446 nm, which represents the intrinsic fluorescence from CNPs.

The photostability of CNPs, which could be an issue in fluorescence imaging, was also investigated. We observed insignificant decay in the fluorescent intensity upon incubation of the functionalised CNPs at 95 °C for 1 h. In addition to exhibiting heat resistance, the CNPs showed negligible photobleaching after continuous exposure to a fluorescent lamp (18 W, 380–760 nm) for >2 weeks (Fig. 6). Interestingly, an increase in fluorescence intensity was observed at 446 nm as the concentration of the $d(AT)_{15}$ oligonucleotide was increased, as shown in Fig. 7a. Concurrently, under blue-light (excitation at 470 nm) illumination, the fluorescence originated solely from CNPs, with no change detected when oligonucleotides were added. The high fluorescence is ascribed to an increased amount of extracted CNPs, with a maximum extraction at 100 μM of $d(AT)_{15}$ (Fig. 7b). To further investigate the effect of

nucleotide composition on the extraction efficiency, we simplified the oligonucleotide sequences by employing ssDNAs

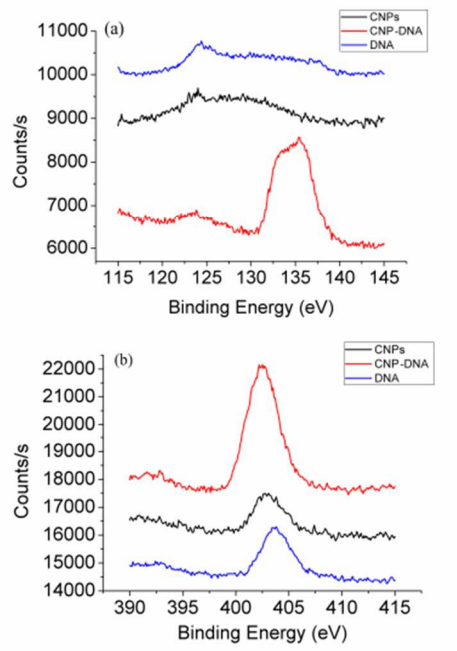

Fig. 4 XPS spectra of elemental (a) P and (b) N in bare CNPs, ssDNA, and oligonucleotide-functionalised CNP (CNP–DNA) samples.

that were 12 bases in length and comprised homogeneous nucleobases dA (adenine), dG (guanine), dC (cytosine), and dT (thymine). The results, shown in Fig. 8, indicate the CNP extraction efficiency varied in the following order: $d(A)_{12} > d(C)_{12} > d(G)_{12} > d(T)_{12}$. The facilitated extraction of fluorescent CNPs by oligonucleotides can be attributed to the π–π interaction between individual nucelobases and the sp^2 carbon atoms on the surfaces of CNPs. Previous studies investigating nucleobase adsorption isotherms on carbon nanotubes and *ab initio* calculations using graphene[27,28] showed that the two aromatic rings of dG and dA purines have higher binding affinities than those of the single aromatic ring dC and dT pyrimidines. In our study, the interaction of nucleobases with CNPs exhibited discrepancies from such reported phenomena. We speculate that the disparity observed in our binding profile may have been the result of CNP curvatures, which effectively determine the binding energy.[27] In addition, we found that the lengths of individual π–π nucleobases adsorbing on the carbon-nanotube surface were typically in the range of 3.3–3.8 Å,[29] which are similar to what has been reported for neighbouring planes in graphite and the length between hydrogen-bond donor atoms and the centroid of an aromatic ring (3.2–3.8 Å).[30,31]

The highest extraction efficiency for the CNP–$d(A)_{12}$ complex can be explained by its orientation, which may have enabled both NH–π and π–π stacking interactions. Consequently, we propose a hypothetical binding mechanism of the CNP–oligonucleotide complex, as shown in Scheme 2. Here, the $–NH_2$ functional group located at the C-6 position of the adenine ring and the C-4 position of cytosine bases may act as a H donor, forming π–H bonds with the aromatic system of the CNP surface, thus stabilising the complex. In contrast, the carbonyl group at the C-6 position of guanine and the C-4 position of thymine, with electron-rich C=O oxygen and aryl-ring π electrons at the CNP surface, is expected to induce repulsion.[32] Additionally, the steric hindrance of the methyl group at the C-5 position of thymine may have worsened the stability of the final complex, resulting in the atypical extraction efficiencies observed among the different nucleobases examined.

Using the current experimental setup, we further examined whether oligonucleotide conformation and length influenced the observed dispersion, fluorescence intensity, and extraction efficiencies. For this purpose, several ssDNA sequences were employed, with initial studies conducted using sequences with either 30 or 45 bases. Our preliminary findings indicated a higher extraction efficiency and fluorescence intensity for the oligonucleotide with 30-mer (ESI Fig. S1†) compared to that with 45-mer (although we could not exclude the potential influence of different random nucleobase compositions at this stage).

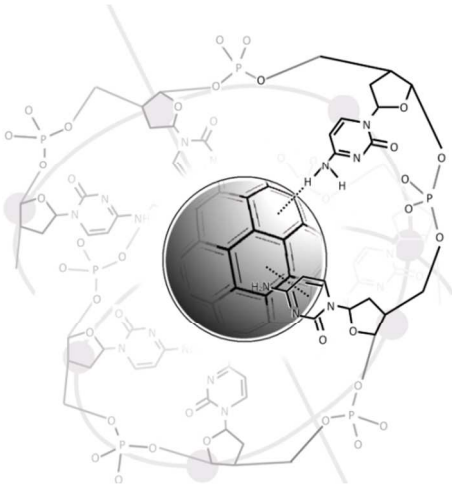

Scheme 2 Proposed interaction between the nucleobases and CNP. (Note: To clearly demonstrate the surface interaction, the figure is not drawn to scale.) The proposed binding mechanism can be attributed to NH–π interaction and π–π stacking at the interface. (The amino group at the C-4 position of cytosine in this figure may serve as a H donor.)

A similar phenomenon was also observed in the linearised plasmid double-strand DNA (dsDNA), which displayed inferior enrichment and lower fluorescence intensity compared with either short dsDNA or ssDNA (Fig. S1). The short, linear ssDNA provided significant improvement for CNP-extraction and was highly fluorescent. An alternative explanation for such behaviour involves steric hindrance, which can diminish interactions between long oligonucleotides and relatively small CNPs (~2 nm). The dsDNA possesses buried base pairs in the double helix structure with limited π–π and π–H bond interactions between nucleotides and CNPs; consequently, it was unable to extract CNPs as effectively as ssDNA. The relative stability and importance of H-bonded and stacked structures represent a considerable complexity of the binding mechanism. Experimental and theoretical studies reported by Braun *et al*.[33] indicated surprisingly stable π–π stacked and NH–π H-bonded structures of the benzene–indole complex, which strongly support our hypothesis of binding forces between nucleobases and CNP surfaces contributing to a favourable interaction. The interactions between oligonucleotides and carbon nanoparticles with such small sizes are yet to be elucidated. To the best of our knowledge, this is the first study exploring the interface between carbon nanoparticles and oligonucleotides. Detailed theoretical simulations are underway to confirm our findings.

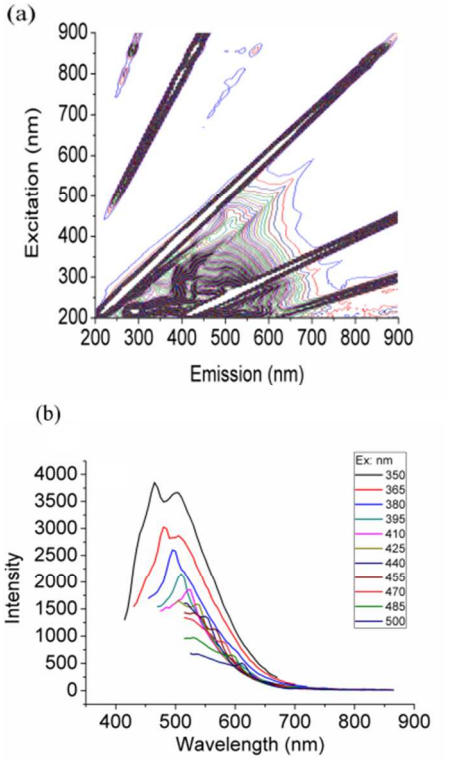

Fig. 5 (a) 3D fluorescence spectra of extracted CNPs (full scan of excitation and emission at wavelengths in the range of 200–900 nm). The denser the lines, the more intense the fluorescence. The maximal excitation wavelength of CNPs was located in the UV region, and the corresponding maximal emission wavelength was near 400–450 nm. (b) The fluorescence emission of CNPs was excitation-dependent.

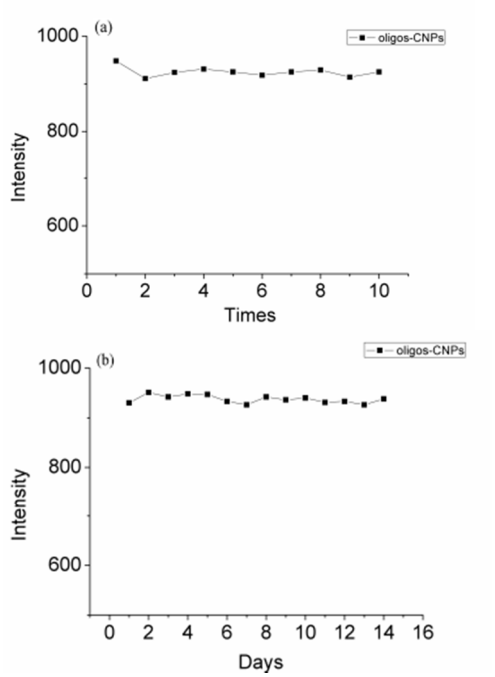

Fig. 6 Fluorescence intensity of oligonucleotide-functionalised CNPs (a) at 95 °C and (b) under a halogen lamp for 14 days.

Previous reports[10,34] have shown that CNPs can serve as ideal cell-imaging probes owing to their biocompatibility and low cytotoxicity. To demonstrate biological applications of CNPs, we employed CLSM to monitor HCT116 cells that were treated with oligonucleotide-functionalized CNPs and HCT116 cells that were untreated. After washing away the residual CNP probes, bright-field and fluorescence images were taken simultaneously by the CLSM using blue-light excitation (405 nm). Results revealed that incubation of the cells with oligonucleotide-functionalized CNPs for 30 min was sufficient for uptake of the CNPs. As shown in Fig. 9b, e-g, HCT116 cells treated with oligonucleotide-functionalised CNPs emitted green fluorescence intracellularly upon excitation, whereas the control (untreated) cells appeared to be unstained (Fig. 9d, h-j). This implies that the CNPs were able to penetrate the cells easily and could be readily monitored using visible excitation. Overnight incubation (24 h) of cells with CNPs also revealed no cytotoxicity and negligible decay in fluorescence (ESI Fig. S2[†]).

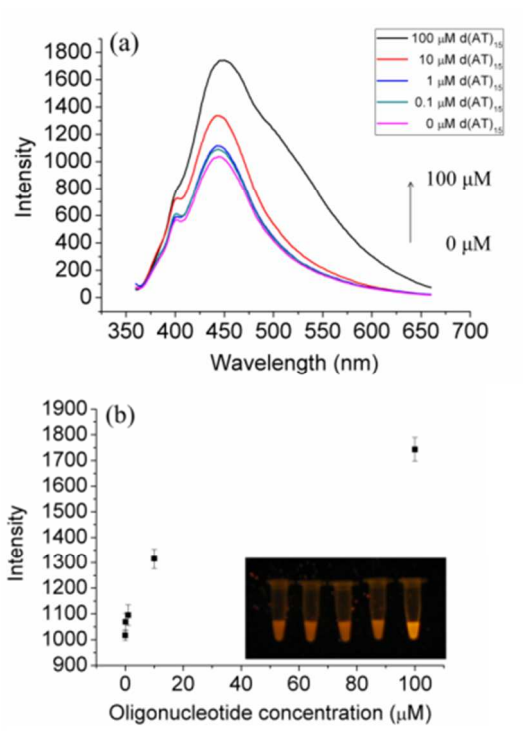

Fig. 7 Dependence of extraction efficiency of CNPs on oligonucleotide concentration. The green-yellow fluorescence of CNPs was observed by direct excitation under blue-light illumination. (a) Increase in fluorescence emission at 446-nm band owing to increasing $d(AT)_{15}$ concentration. (b) The extraction maximum was achieved at a concentration of 100 μM.

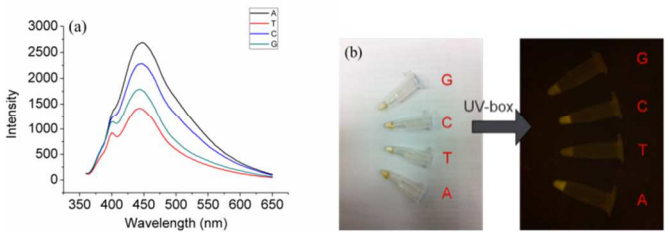

Fig. 8 Nucleobase-dependent extraction efficiency of CNPs. (a) The increase in fluorescence emission at the 446-nm band indicates the presence of a large amount of extracted CNPs. Varying CNP-extraction efficiencies were observed in the following order: $d(A)_{12}$ > $d(C)_{12}$ > $d(G)_{12}$ > $d(T)_{12}$. (b) Green-yellow fluorescence emission of CNPs was identified by direct excitation under blue-light illumination.

The π–π stacking and π–HN interactions at the interface of oligonucleotide-CNPs can presumably improve their water solubility. The fluorescent CNPs extracted in this study were effectively bound to ssDNA. Previous reports have shown that biological activities are largely retained in DNA-bound carbon nanotubes.[21] Owing to the low toxicity of our ssDNA-capped CNPs (Fig. 10), the functionalisation of CNPs with an appropriate sequence may allow more precise control of the interfacial properties for specific applications. Moreover, this enables an alternative strategy for the development of novel label-free biosensors with which selective detection of nucleic acids can be achieved (ESI Fig. S3†) by simply monitoring the fluorescent intensities of tagged CNPs.

In the present study, our goal is to provide a universal approach using oligonucleotides as both the solvent and stabilising agent to enable *in situ* extraction and functionalisation of CNPs. Such strategy is expected to be applicable to any top-down method to perform downstream CNP extraction and functionalisation. The oligonucleotides themselves improve the hydrophilicity of the carbon nanomaterials and may serve as great adsorbents to positively charged ligands for further layer-by-layer (LbL) surface modification in diverse drug delivery systems or biosensor applications…etc. It is also important to note that we were also able to easily re-suspend precipitated SWCNTs using DI water (ESI Fig. S4†). Because the photoluminescence intensity can be dramatically reduced by aggregation of purified nanotubes, isolated SWCNTs with retained dispersibility may be useful in various applications. Thus, our one-pot process is capable of generating two different types of functionalised carbon nanomaterials simultaneously. Moreover, the distinct light-emitting properties of these CNPs allow them to be distinguished from SWCNTs (CNPs synthesised in this study emitted fluorescence at ~450 nm (λ_{ex} = 405 nm), whereas typical SWCNTs are known to fluoresce within the NIR region[3]). This suggests a simple approach to characterise dispersed SWCNTs is yet to be explored.

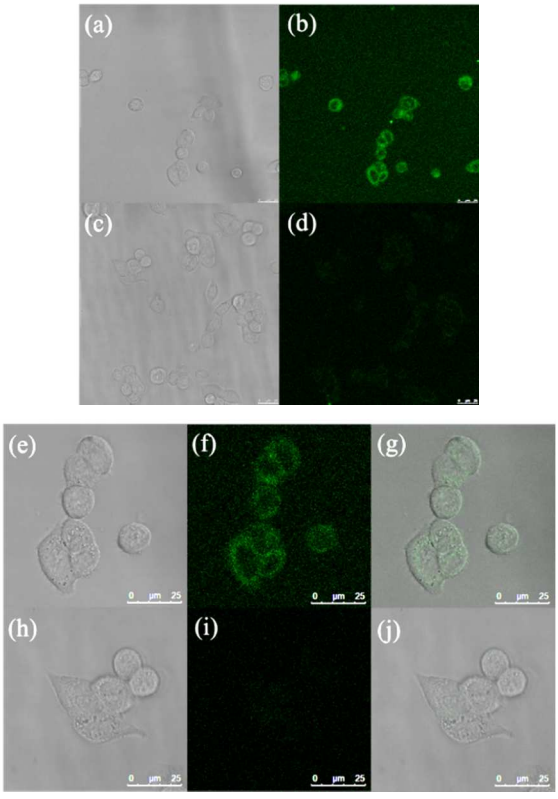

Fig. 9 CLSM images under (a) bright field and (b) blue-light excitation (405 nm) of HCT116 cells that were treated with oligonucleotide-functionalised CNPs for 30 min. Images of untreated HCT116 cells under (c) bright field and (d) blue-light excitation. HCT116 cells that were treated with oligonucleotide-functionalised CNPs emitted green fluorescence upon 405-nm excitation; untreated control cells appeared to be unstained. ((e), (f), (h) and (i) are 4x magnified images from (a), (b), (c) and (b) respectively; (g) is the overlay of (e) and (f); (j) is the overlay of (h) and (i); scale bar= 25 μm)

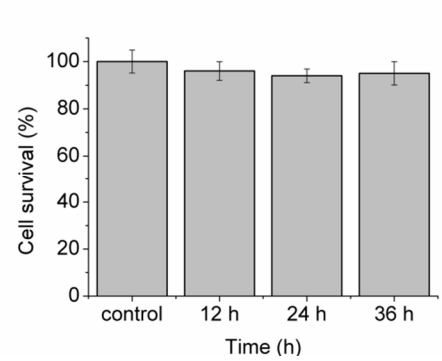

Fig. 10 Evaluation of the oligonucleotide-functionalised CNPs' toxicity by MTT assay. After 36 h of incubation, no significant cell death was observed. (Control cells were cultured in DMEM medium without additional treatments.)

Conclusion

We successfully developed a one-step method for the extraction and functionalisation of fluorescent CNPs (with diameter ≈ 2 nm) from acid-treated SWCNTs. This novel method improves and simplifies the conventional synthesis processes employed for CNP preparation, which often involve additional steps of surface functionalisation, neutralisation, and dialysis. The use of oligonucleotides in our study enhanced the extraction of CNPs from acid-treated SWCNTs. Moreover, the fluorescent CNPs remained stable under ambient conditions for several months and were shown to be applicable for cell imaging owing to negligible photobleaching effects. However, the fluorescence emitted at shorter wavelength (400–600 nm) from the synthesized CNPs may encounter the issue of autofluorescence in tissues when utilized *in vivo*. It can be resolved by implementing other top-down procedures or using other carbon precursors to alter the intrinsic fluorescence of CNPs, followed by our bio-solvent-extraction strategy. Investigations using specific oligonucleotides such as aptamers and siRNAs are also currently underway to develop CNPs that can function as highly specific bio-sensors and versatile transfection reagents or drug carriers. For the latter, real-time imaging of drug-delivery efficiency can easily be achieved by directly monitoring fluorescent CNPs.

Acknowledgements

This work was supported by the National Science Council of Taiwan (Grants No. NSC 99-2113-M-009-016-MY2) and the Ministry of Education, Taiwan ('Aim for the Top University Plan' of National Chiao Tung University).

Notes and references

Department of Applied Chemistry and Institute of Molecular Science, National Chiao-Tung University, No.1001 Ta-Hsueh Road, Hsinchu 30010, Taiwan. E-mail: hyhsu99@nctu.edu.tw; Tel: +886-(0)3-5712121, ext. 56556

The authors declare no competing financial interest.

† Electronic Supplementary Information (ESI) available. See DOI: 10.1039/b000000x/

1. W. Zhou, Y. H. Ooi, R. Russo, P. Papanek, D. E. Luzzi, J. E. Fischer, M. J. Bronikowski, P. A. Willis and R. E. Smalley, *Chem. Phys. Lett.*, 2001, **350**, 6–14.
2. J. Zhang, A. A. Boghossian, P. W. Barone, A. Rwei, J. H. Kim, D. Lin, D. A. Heller, A. J. Hilmer, N. Nair, N. F. Reuel and M. S. Strano, *J. Am. Chem. Soc.*, 2011, **133**, 567–581.
3. K. Welsher, Z. Liu, D. Daranciang and H. Dai, *Nano Lett.*, 2008, **8**, 586–590.
4. X. Michalet, F. F. Pinaud, L. A. Bentolila, J. M. Tsay, S. Doose, J. J. Li, G. Sundaresan, A. M. Wu, S. S. Gambhir and S. Weiss, *Science*, 2005, **307**, 538–544.
5. M. Bruchez, Jr., M. Moronne, P. Gin, S. Weiss and A. P. Alivisatos, *Science*, 1998, **281**, 2013–2016.
6. I. H. El-Sayed, X. Huang and M. A. El-Sayed, *Nano Lett.*, 2005, **5**, 829–834.
7. H. Liu, T. Ye and C. Mao, *Angew. Chem.*, 2007, **46**, 6473–6475.
8. X. Xu, R. Ray, Y. Gu, H. J. Ploehn, L. Gearheart, K. Raker and W. A. Scrivens, *J. Am. Chem. Soc.*, 2004, **126**, 12736–12737.
9. M. Bottini, C. Balasubramanian, M. I. Dawson, A. Bergamaschi, S. Bellucci and T. Mustelin, *J. Phys. Chem. B*, 2006, **110**, 831–836.
10. S. C. Ray, A. Saha, N. R. Jana and R. Sarkar, *J. Phys. Chem. C*, 2009, **113**, 18546–18551.
11. Y. Fang, S. Guo, D. Li, C. Zhu, W. Ren, S. Dong and E. Wang, *ACS Nano*, 2012, **6**, 400–409.
12. Y. P. Sun, B. Zhou, Y. Lin, W. Wang, K. A. Fernando, P. Pathak, M. J. Meziani, B. A. Harruff, X. Wang, H. Wang, P. G. Luo, H. Yang, M. E. Kose, B. Chen, L. M. Veca and S. Y. Xie, *J. Am. Chem. Soc.*, 2006, **128**, 7756–7757.
13. M. A. Hamon, M. E. Itkis, S. Niyogi, T. Alvaraez, C. Kuper, M. Menon and R. C. Haddon, *J. Am. Chem. Soc.*, 2001, **123**, 11292–11293.
14. M. E. Itkis, D. E. Perea, R. Jung, S. Niyogi and R. C. Haddon, *J. Am. Chem. Soc.*, 2005, **127**, 3439–3448.
15. J. A. Fagan, B. J. Landi, I. Mandelbaum, J. R. Simpson, V. Bajpai, B. J. Bauer, K. Migler, A. R. Walker, R. Raffaelle and E. K. Hobbie, *J. Phys. Chem. B*, 2006, **110**, 23801–23805.
16. S. Lebedkin, F. Hennrich, T. Skipa and M. M. Kappes, *J. Phys. Chem. B*, 2003, **107**, 1949–1956.
17. S.-L. Hu, K.-Y. Niu, J. Sun, J. Yang, N.-Q. Zhao and X.-W. Du, *J. Mater. Chem.*, 2009, **19**, 484–488.
18. Q.-L. Zhao, Z.-L. Zhang, B.-H. Huang, J. Peng, M. Zhang and D.-W. Pang, *Chem. Commun. (Cambridge, U. K.)*, 2008, 5116–5118.
19. S. Zhang, Q. He, R. Li, Q. Wang, Z. Hu, X. Liu and X. Chang, *Mater. Lett.*, 2011, **65**, 2371–2373.
20. W. Lu, X. Qin, S. Liu, G. Chang, Y. Zhang, Y. Luo, A. M. Asiri, A. O. Al-Youbi and X. Sun, *Anal. Chem.*, 2012, **84**, 5351–5357.
21. F. Lu, L. Gu, M. J. Meziani, X. Wang, P. G. Luo, L. M. Veca, L. Cao and Y.-P. Sun, *Adv. Mater.*, 2009, **21**, 139–152.
22. Z. Guo, J. Ren, J. Wang and E. Wang, *Talanta*, 2011, **85**, 2517–2521.
23. M. Zheng, A. Jagota, E. D. Semke, B. A. Diner, R. S. Mclean, S. R. Lustig, R. E. Richardson and N. G. Tassi, *Nat. Mater.*, 2003, **2**, 338–342.
24. J. Liu, A. G. Rinzler, H. Dai, J. H. Hafner, R. K. Bradley, P. J. Boul, A. Lu, T. Iverson, K. Shelimov, C. B. Huffman, F. Rodriguez-Macias, Y. S. Shon, T. R. Lee, D. T. Colbert and R. E. Smalley, *Science*, 1998, **280**, 1253–1256.
25. H. Li, J. Zhai, J. Tian, Y. Luo and X. Sun, *Biosens. Bioelectron.*, 2011, **26**, 4656–4660.
26. R. R. Lahiji, B. D. Dolash, D. E. Bergstrom and R. Reifenberger, *Small*, 2007, **3**, 1912–1920.
27. D. Umadevi and G. N. Sastry, *J Phys Chem Lett*, 2011, **2**, 1572–1576.
28. R. R. Johnson, A. T. C. Johnson and M. L. Klein, *Nano Lett.*, 2007, **8**, 69–75.
29. Z. Xiao, X. Wang, X. Xu, H. Zhang, Y. Li and Y. Wang, *J. Phys. Chem. C*, 2011, **115**, 21546–21558.
30. L. M. Salonen, M. Ellermann and F. Diederich, *Angew. Chem.*, 2011, **50**, 4808–4842.
31. S. Tsuzuki, K. Honda, T. Uchimaru, M. Mikami and K. Tanabe, *J. Am. Chem. Soc.*, 2000, **122**, 11450–11458.
32. M. Egli and S. Sarkhel, *Acc. Chem. Res.*, 2006, **40**, 197–205.
33. J. Braun, H. J. Neusser and P. Hobza, *J. Phys. Chem. A*, 2003, **107**, 3918–3924.
34. M. Kawaguchi, J. Ohno, A. Irie, T. Fukushima, J. Yamazaki and N. Nakashima, *Int. J. Nanomedicine*, 2011, **6**, 729–736.

TOC Graphic and entry

We used ssDNA oligonucleotide as a 'bio-solvent' for CNP extraction and *in situ* functionalisation, developing efficient, eco-friendly, biocompatible fluorescence probes.